

Multiple Mechanisms in Pd(II)-Catalyzed S_N2' Reactions of Allylic Alcohols

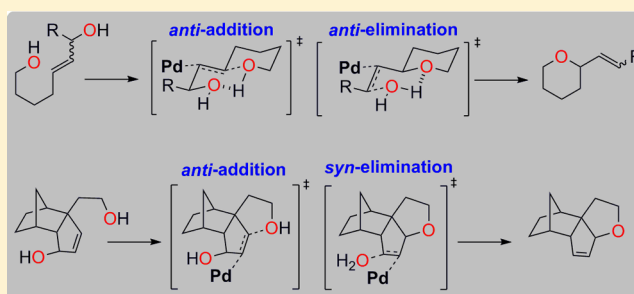
Thomas Ghebregiorgis,[‡] Brian H. Kirk,[†] Aaron Aponick,^{*,‡} and Daniel H. Ess^{*,†}

[†]Department of Chemistry and Biochemistry, Brigham Young University, Provo, Utah 84602, United States

[‡]Department of Chemistry, University of Florida, Gainesville, Florida 32611, United States

S Supporting Information

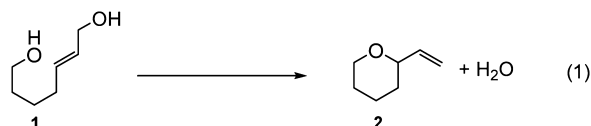
ABSTRACT: Density functional calculations and experiments were used to examine mechanisms of Pd(II) catalyzed intramolecular cyclization and dehydration in acyclic and bicyclic monoallylic diols, a formal S_N2' reaction. In contrast to the previously proposed *syn*-oxypalladation mechanism for acyclic monoallylic diols, calculations and experiments strongly suggest that hydrogen bonding templates a hydroxyl group and Pd addition across the alkene and provides a low energy pathway via *anti*-addition (*anti*-oxypalladation) followed by intramolecular proton transfer and *anti*-elimination of water. This *anti*-addition, *anti*-elimination pathway also provides a simple rationale for the observed stereospecificity. For bicyclic monoallylic diol compounds, Pd(II) is capable of promoting either *anti*- or *syn*-addition. In addition, palladium chloride ligands can mediate proton transfer to promote dehydration when direct intramolecular proton transfer between diol groups is impossible.



INTRODUCTION AND BACKGROUND

Lewis acids have played a prominent role in the progression of the field of organic synthesis.¹ Examples range from Friedel–Crafts alkylation² to enantioselective Diels–Alder reactions.³ The substrates for these reactions typically interact with Lewis acids at heteroatoms such as oxygen, nitrogen, or halogen. More recently, a tremendous amount of effort has been focused on using carbophilic metal complexes to activate C–C π -bonds.⁴ While there are many classic examples, such as oxymercuration, there has recently been a surge in this area due to the development of environmentally benign and less toxic reagents. Examples include Au, Pt, and Pd complexes.⁵

Successful development of new transformations relies on the ability to predict the site of reactivity and mode by which Lewis acids activate substrates. However, significant difficulties can be encountered when a catalyst can function either as a traditional hard Lewis acid or as a carbophilic soft Lewis acid.⁶ Herein we report on just such a catalytic system that can activate an allylic alcohol through the olefin, hydroxyl group, or both in an intramolecular cyclization reaction (eq 1).⁷



As can be seen in eq 1, the reaction involves the addition of a hydroxyl nucleophile to an allylic system, generating water as the byproduct. Substitution reactions of unactivated allylic systems have been increasingly reported,⁸ and several different

mechanistic scenarios can be operative including cationic, π -allylmetal, S_N2' , and stepwise formal S_N2' pathways.⁹ Our interest in this reaction stems from the discovery by Aponick and co-workers that Au(I)-salts are highly effective catalysts for the transformation.¹⁰ Other catalysts based on complexes of Fe(III), Bi(III), Pd(0), Pt(0), Rh(I), Ru(II), and Pd(II) have been reported, with the proposed mechanism differing according to identity and oxidation state of the metal complex employed.⁸

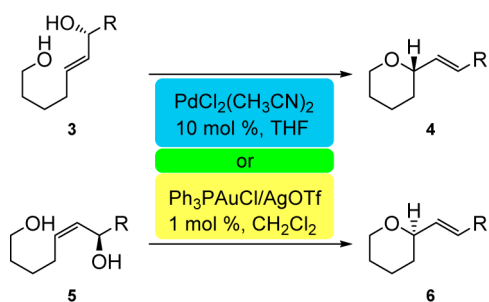
We have previously reported on the chirality transfer in Au(I)-catalyzed cyclization of nonracemic allylic alcohol substrates and performed extensive experiments and theoretical studies to understand the mechanism.¹¹ Prior to our work with Au(I), Uenishi and co-workers showed that Pd(II) complexes also catalyze the stereospecific formation of pyrans from acyclic monoallylic diols.^{7,8f} Scheme 1 compares the experimental conditions for Au(I) and Pd(II) catalyzed cyclization and dehydration. The reactions are highly effective with both sets of conditions, 10 mol % PdCl₂(CH₃CN)₂ in THF or 1 mol % Ph₃PAuCl/AgOTf in CH₂Cl₂, and in all cases the chirality of the allylic alcohol is transferred to the newly formed stereocenter. This chirality transfer happens with the same absolute sense and is consistent over a wide range of examples.

Au(I) complexes are generally presumed to be soft carbophilic metals that coordinate with olefins to form linear π -complexes.¹² Pd(II) complexes are typically harder Lewis acids than Au(I) and can function by activating either C–C π -

Received: June 8, 2013

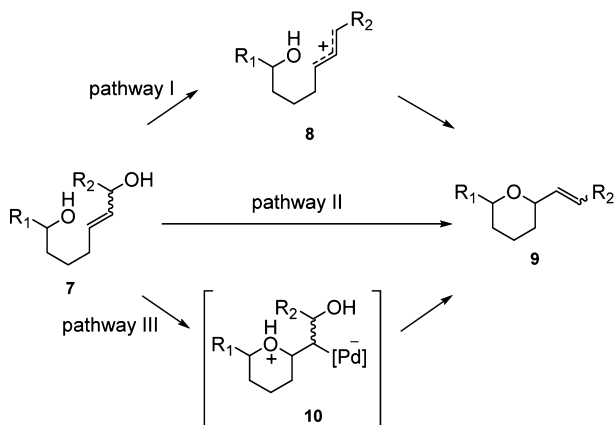
Published: July 17, 2013

Scheme 1. General Conditions for Monoallylic Diol Cyclization and Dehydration



bonds or heteroatoms.¹³ Additionally, Pd(II) complexes accommodate more ligands than Au. These features of Pd(II) potentially increase the complexity of the mechanism, but there are three general mechanisms for Pd(II) catalyzed cyclization and dehydration of monoallylic diol **7** (Scheme 2). The transformation is a formal S_N2' process, and pathway I involves formation of a π -allylation via Pd induced hydroxide loss, which can then undergo cyclization with the remaining nonallylic hydroxyl group. Pathway II involves either a *syn* or *anti* concerted S_N2' process that features simultaneous C–O bond formation with water loss. Pathway III involves stepwise alkene oxypalladation to give a Pd–C σ alkyl species followed by water elimination. Pathway III can occur by either *syn*- or *anti*-oxypalladation followed by subsequent *syn*- or *anti*-elimination of water. This pathway is also complicated by the potential for HCl to be generated, either before or after cyclization. HCl has the potential to act as a Brønsted acid catalyst for cyclization and dehydration.

Scheme 2. Possible Cyclization and Dehydration Mechanisms

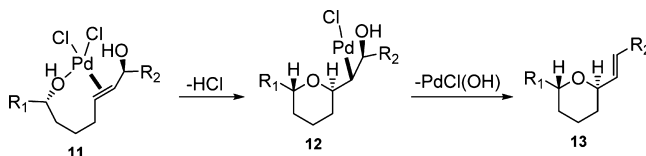


In our previous work with Au(I) phosphine catalysts we identified the *anti*-addition, *anti*-elimination (in reference to the relationship between the Au-catalyst and the hydroxyl nucleophile) as the preferred mechanism due to the influence of the diol hydrogen bonding and preference for Au(I) to act as a π acid and remain linear and divalent.^{11b} However, it is well-known that Pd(II) can promote either *syn*- or *anti*-addition to alkenes.¹⁴ For example, Stahl and co-workers have reported competitive *syn*- and *anti*-addition pathways for Pd catalyzed intramolecular oxidative amination of alkenes.¹⁵ In fact, Uenishi proposed a *syn*-addition (i.e., *syn*-oxypalladation) and *syn*-

elimination of water with a stereocontrol model based on allylic strain relief.^{7,8f}

The proposed Uenishi *syn* S_N2' mechanism begins with coordination of *cis*-PdCl₂ to the alkene and hydroxyl group to give complex **11** (Scheme 3).^{7,8f} Subsequent *syn*-oxypalladation

Scheme 3. Simplified Uenishi *syn* S_N2' Mechanism



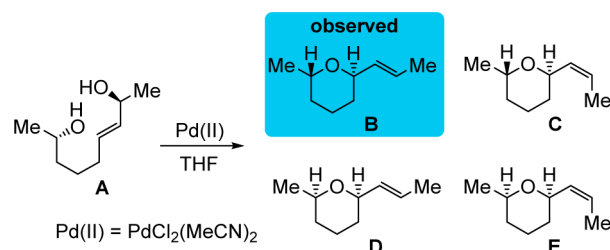
and HCl loss results in the Pd–C σ alkyl species **12** that then undergoes *syn*-elimination to give PdCl(OH) and the pyran product **13**. Uenishi suggested that in subsequent catalytic cycles PdCl(OH) might act as an active catalyst or PdCl₂ can be regenerated by reaction of PdCl(OH) with HCl.^{8f}

Herein we report density functional theory (DFT) calculations and experiments that examine the mechanism of Pd(II) catalyzed S_N2' reactions of acyclic and bicyclic monoallylic diols. In contrast to the proposed *syn*-addition, *syn*-elimination pathway, our studies reveal that the lowest energy pathway for acyclic monoallylic diols occur via *anti*-oxypalladation followed by *anti*-elimination of water with PdCl₂(MeCN) acting as the active catalyst. This pathway is similar to the mechanism identified for Au(I) catalysis and provides a simple rationale for stereocontrol. Different from Au(I) catalysis, we demonstrate that in bicyclic monoallylic diol systems where *anti*-oxypalladation is high in energy *syn*-oxypalladation can proceed. Also, we show that Pd(II) is capable of providing a novel *anti*-addition, *syn*-elimination mechanism for the cyclization and dehydration of a bicyclic compound where Au fails to catalyze cyclization.

RESULTS AND DISCUSSION

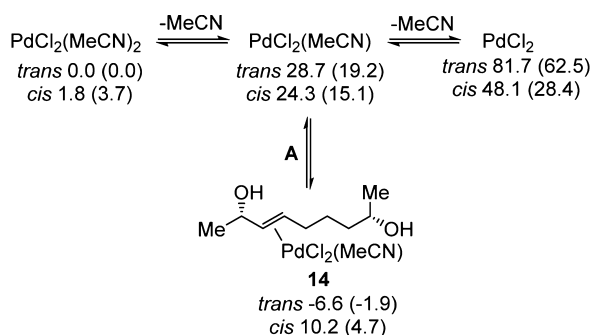
Observed Stereoselectivity. For computational exploration of the cyclization and dehydration mechanism of acyclic compounds we examined monoallylic diol stereoisomer **A** (Scheme 4). Uenishi reported that **A** cyclizes in the presence of

Scheme 4. Possible Stereoisomer Products from Pd(II) Catalyzed Cyclization and Dehydration



catalytic amounts of PdCl₂(MeCN)₂ leading selectively to only diastereoisomer **B**.^{7,8f} Uenishi has also reported the stereoselective cyclization of the three alternative stereoisomers of **A**.^{7,8f} Calculations on the alternative stereoisomers were performed and do not alter the mechanism or model of stereoselectivity and so are not presented here.

Entry into the Catalytic Cycle. To begin, we computationally examined the possible coordination thermodynamics of PdCl₂(MeCN)₂ with monoallylic diol **A** (Scheme 5). Although

Scheme 5. Enthalpy (Free Energy) of Precatalyst Species and Entry Point into the Catalytic Cycle (kcal/mol)^a

^a*Trans* and *cis* refer to relative configuration of chloride ligands.

the *trans*- $\text{PdCl}_2(\text{MeCN})_2$ complex is 1.8 kcal/mol more stable than the *cis*- $\text{PdCl}_2(\text{MeCN})_2$ complex, after acetonitrile loss the *cis*- $\text{PdCl}_2(\text{MeCN})$ complex is 4.4 kcal/mol more stable due to the preference for chloride to orient *trans* to a vacant coordination site. There is a $\Delta H = 24.3$ kcal/mol and $\Delta G = 15.1$ kcal/mol penalty to achieve the *cis*- $\text{PdCl}_2(\text{MeCN})$ complex. The loss of a second acetonitrile ligand to give PdCl_2 with two vacant coordination sites is unlikely and is endothermic by >48 kcal/mol. This suggests that monoallylic diol **A** coordinates to $\text{PdCl}_2(\text{MeCN})$ to enter into the catalytic cycle. Exploration of possible coordination modes for **A** with $\text{PdCl}_2(\text{MeCN})$ shows that the most favorable coordination occurs with the π bond rather than hydroxyl groups and with the chlorides in a *trans* configuration. The *trans*- $\text{PdCl}_2(\text{MeCN})$ -(**A**) complex (**14**, Scheme 5) is exothermic by -6.6 kcal/mol relative to *trans*- $\text{PdCl}_2(\text{MeCN})_2$. This suggests that once the catalytic cycle has begun $\text{PdCl}_2(\text{MeCN})_2$ is likely off cycle.

Pathways I and II. For pathway I (Scheme 2), starting at complex **14** the computed ΔH for $\text{PdCl}_2(\text{MeCN})$ induced ionization of the allylic hydroxyl group is ~ 50 kcal/mol. This high energy, coupled with the experimental stereochemical transfer for the conversion of **A** into **B** (Scheme 4), suggests that this carbocationic pathway can be ruled out.

Pathway II provides stereochemical transfer by either a *syn* or *anti* concerted $\text{S}_{\text{N}}2'$ process. Although this is generically shown in Scheme 2, there are several distinct stereochemical possibilities illustrated in Scheme 6. The *syn* and *anti* $\text{S}_{\text{N}}2'$ labels in Scheme 6 refer to the relative orientation of the incoming hydroxyl nucleophile and the outgoing leaving group.

There are two potential types of transition states for concerted *syn* $\text{S}_{\text{N}}2'$ pathways that can be envisioned, which differ by whether Pd coordinates with the hydroxyl leaving group or π bond. However, no concerted transition states were located with $\text{PdCl}_2(\text{MeCN})$ coordination to the π bond. The concerted *syn* $\text{S}_{\text{N}}2'$ transition state, **ConcTS**, is shown in Figure 1. This transition state features simultaneous C–O bond formation and hydroxyl group loss mediated by the Pd. Although this transition state involves diol hydrogen bonding, the $\Delta H^\ddagger = 28.0$ kcal/mol relative to complex **14** is too high to be consistent with the low temperatures reported by Uenishi.^{7,8f} The large ΔH^\ddagger is likely due to the poor leaving group ability of hydroxide that is not fully compensated for by the palladium catalyst. We have also explored the possibility of intramolecular diol proton transfer prior to concerted *syn* $\text{S}_{\text{N}}2'$, but the energetic cost of proton transfer makes this pathway prohibitive.

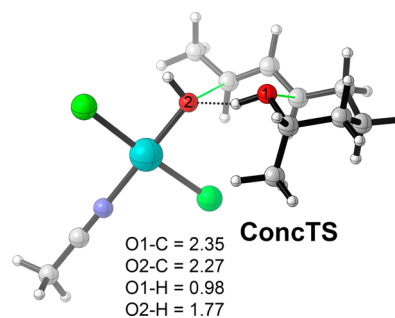
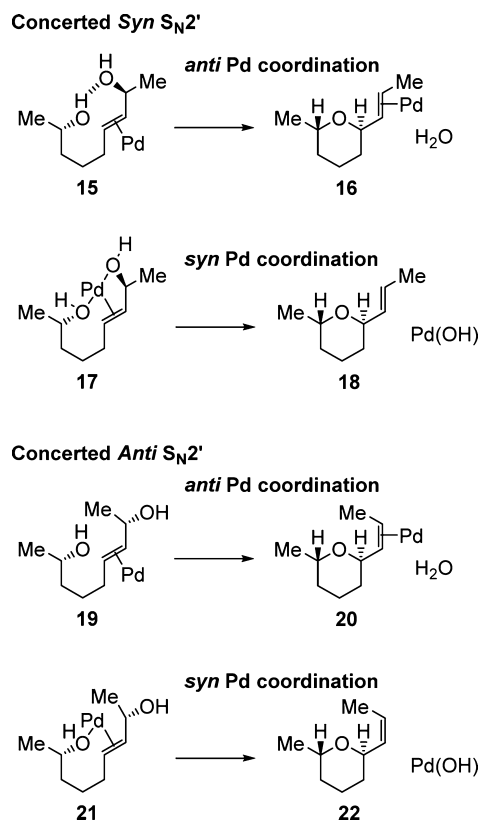
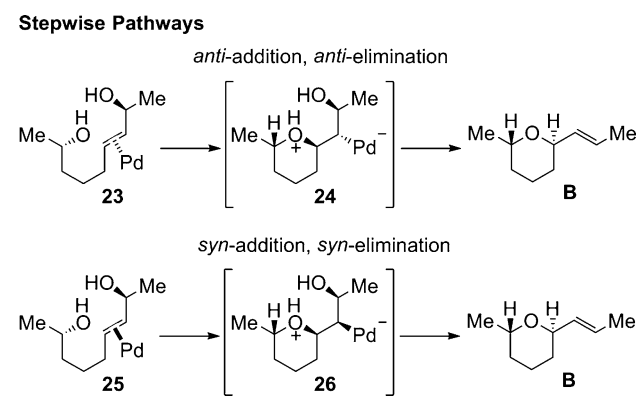
Scheme 6. Possible *syn* and *anti* Concerted $\text{S}_{\text{N}}2'$ Mechanisms

Figure 1. Concerted *syn* $\text{S}_{\text{N}}2'$ transition state. Bond lengths reported in Å.

Importantly, concerted *anti* $\text{S}_{\text{N}}2'$ pathways cannot lead to the pyran stereoisomer **B**. Concerted *anti* $\text{S}_{\text{N}}2'$ can only lead to stereoisomer **C** with a *cis* alkene unit. However, for this pathway to occur there can be no diol hydrogen bonding, which involves a higher energy transition state than **ConcTS**.

Pathway III: Stepwise Addition (Oxypalladation) and Elimination. From complex **14** there are two general cyclization and dehydration pathways that involve stepwise oxypalladation and elimination of water that arrive at the experimentally observed product (Scheme 7). The *anti*-addition, *anti*-elimination pathway involves coordination of the palladium catalyst on the π face opposite to both the incoming nucleophile and departing leaving group. In this pathway the diol groups also have the possibility of hydrogen bonding. Upon cyclization of **23**, σ -complex **24** results. From **24**, proton transfer and water expulsion also occur *anti* to Pd. Because the Pd catalyst remains *anti* to the hydroxyl groups

Scheme 7. Illustration of Stepwise Addition and Elimination Pathways



throughout this pathway there is no possibility for palladium hydroxide formation.

The *syn*-addition, *syn*-elimination pathway involves coordination of the palladium catalyst to the same π face as both the incoming nucleophile and departing hydroxyl group, resulting in the conversion of **25** into intermediate **26**. In this case there is the possibility for the diol groups to maintain hydrogen bonding or for the hydrogen bonding to be disrupted by the Pd catalyst. By this pathway, *syn*-addition forms the Pd–C σ -complex, after which water or HCl and Pd(OH) can be released forming the olefin.

While the *syn*-addition, *syn*-elimination pathway was proposed by Uenishi,^{7,8f} and *syn*-oxypalladation is well-known,¹⁶ the *anti*-addition, *anti*-elimination pathway was found to be lowest in energy under Au(I) conditions.^{11b} With this curious difference between Au and Pd in mind we examined both *anti* and *syn* mechanisms.

Scheme 8 outlines the enthalpy and free energy surfaces for *anti*-addition, *anti*-elimination. Starting from complex **14**, the transition state for *anti*-oxypalladation involving **TS1a** (Figure 2) has $\Delta H^\ddagger = 6.9$ kcal/mol and $\Delta G^\ddagger = 9.1$ kcal/mol. In **TS1a** the forming O–C bond length is 2.02 Å, and the forming Pd–C bond is 2.11 Å. In **TS1a** the PdCl₂(MeCN) has a *trans* dichloride relationship. The barrier for *cis*-PdCl₂(MeCN) is

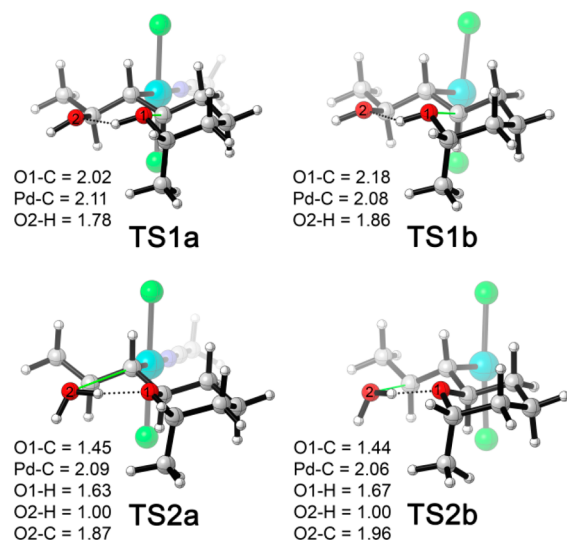


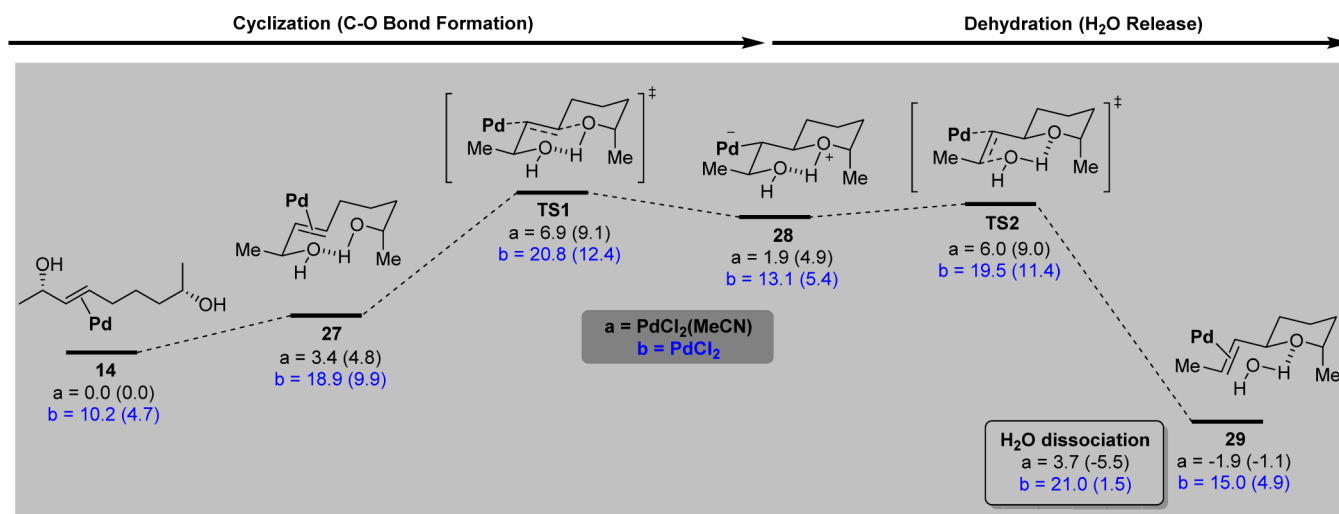
Figure 2. Stepwise cyclization and dehydration transition states. Bond lengths reported in Å.

several kcal/mol higher in energy due to the expected *trans* effect of the forming Pd–C bond.

Key to the low energy of transition state **TS1a** is the nearly full developed Pd–C bond and the diol hydrogen bonding that is close to colinear. Intermediate **28** formed from **TS1a** is endothermic by 1.9 kcal/mol, and the ΔH^\ddagger for proton transfer and water loss is 6.0 kcal/mol via **TS2a** (Scheme 8, Figure 2). In **TS2a** the nonallylic hydroxyl group proton is fully transferred to the allylic hydroxyl group with an O1–H distance of 1.63 Å and an O2–H distance of 1.00 Å. The breaking O2–C bond distance is 1.87 Å. Attempted optimization of structures with proton transfer prior to water loss resulted in reversion back to intermediate **28**. The pyran product **29** involves hydrogen bonding with water and $\Delta H = -1.9$ kcal/mol and $\Delta G = -1.1$ kcal/mol. Complete water loss results in $\Delta G = -5.5$ kcal/mol.

Alternative to **TS1a**, it is possible that prior to cyclization there is loss of the acetonitrile ligand from complex **14**. This has the potential to increase the electrophilicity of Pd resulting in a more activated π bond. Loss of acetonitrile requires $\Delta H =$

Scheme 8. Enthalpy (Free Energy) Reaction Coordinate Diagram (kcal/mol)



10.2 kcal/mol and $\Delta G = 4.7$ kcal/mol. Although this step is energetically reasonable, it does not translate into an overall lower barrier for cyclization and dehydration. The ΔH^\ddagger for cyclization via **TS1b** (Figure 2) is 20.8 kcal/mol and $\Delta G^\ddagger = 12.4$ kcal/mol.

Although the *anti*-addition, *anti*-elimination mechanism is quite feasible, comparison to the calculated *syn*-addition, *syn*-elimination pathway was needed. As discussed earlier, the Uenishi mechanism involves *syn*-oxypalladation followed by *syn*-elimination of PdCl(OH)(HCl).^{8f} Figure 3 shows the

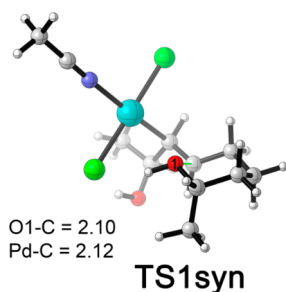


Figure 3. Lowest energy stepwise *syn*-oxypalladation transition state. Bond lengths reported in Å.

lowest energy stepwise *syn*-addition transition state, **TS1syn**. The ΔH^\ddagger for **TS1syn** is 13.5 kcal/mol, which is 6.6 kcal/mol higher than **TS1a**. In **TS1syn** the forming O1–C bond is 2.10 Å and the forming Pd–C bond is 2.12 Å. These values are close to the geometries found in **TS1a**. However, in contrast to **TS1a**, coordination of PdCl₂(MeCN) for *syn*-oxypalladation disrupts intramolecular hydrogen bonding.

We also examined the possibility that *syn*-addition occurs through an anionic mechanism by generation of a Pd-alkoxide species. This involves proton transfer from the nonallylic hydroxyl group to the Pd chloride ligand followed by *syn*-addition of palladium alkoxide to the π bond. However, from **14** intramolecular proton transfer is energetically prohibitive. This suggests that the only reasonable circumstance where HCl can be generated, in the catalysis of acyclic compounds, is after stepwise *syn*-addition. Proton transfer after **TS1syn** from the cyclized pyran to the Pd chloride ligand requires $\Delta H = 4.6$ kcal/mol relative to **14**. Although the thermodynamics for HCl formation are reasonable, the *syn*-addition pathway is too high in energy, relative to the *anti*-addition pathway, to be competitive and therefore production of HCl under catalytic conditions is unlikely.

Transition-State Stereoselectivity. As discussed above, the lowest energy pathway for cyclization and dehydration involves *anti*-addition, *anti*-elimination. This mechanism provides the stereoselective transformation of monoallylic diol **A** into the 2,6-*trans* pyran **B** (Scheme 4). To examine this stereoselectivity we have computed the cyclization transition states leading to the unobserved diastereomers **C**, **D**, and **E**. Although endothermic, the cyclization step is expected to be stereodetermining for both the pyran stereocenter that is formed and also the alkene since the diol hydrogen bonding remains unbroken along the reaction pathway, which templates the stereochemistry of the diastereomer formed.¹¹

Figure 4 shows the lowest energy cyclization transition state, **TS1cis**, leading to pyran stereoisomer **C**. Transition states leading to stereoisomers **D** and **E** are significantly higher in energy. This transition state has $\Delta H^\ddagger = 16.7$ kcal/mol and ΔG^\ddagger

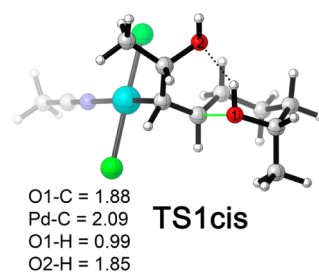


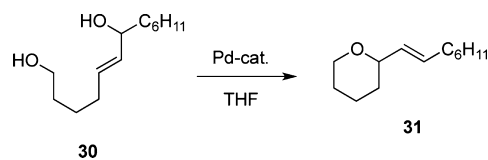
Figure 4. Lowest energy cyclization leading to pyran diastereomer **C**.

= 19.9 kcal/mol. The several kcal/mol higher energy barrier for **TS1cis** versus **TS1a** is mainly the result of 1,3-allylic strain from the orientation of the forming *cis* alkene as well as decreased hydrogen bonding.

Experiments. The calculations reveal several important mechanistic details about the Pd(II) catalyzed allylic cyclization of acyclic monoallylic diols as follows: (1) It is highly likely that one acetonitrile ligand must be lost to form the active catalyst PdCl₂(MeCN), while loss of both acetonitrile ligands is unlikely. (2) Formation of HCl under the reaction conditions may be possible, but would be occurring by an off-cycle pathway. (3) An *anti*-addition, *anti*-elimination mechanism is energetically favored and therefore more accessible than the corresponding *syn*-addition, *syn*-elimination previously proposed for this transformation. To further validate the computational results, we sought to test these concepts experimentally.

To this end, compound **30** was prepared and treated under the conditions listed in Table 1. Entry 1 shows the standard

Table 1. Comparison of Pd Catalysts

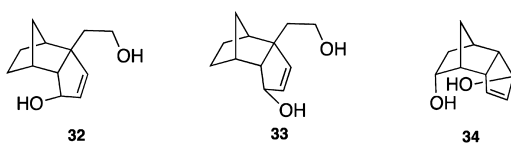


entry	catalyst	temperature	time (h)	yield (%)
1	PdCl ₂ (CH ₃ CN) ₂	0 °C	2.5	92
2 ^a	PdCl ₂ (CH ₃ CN) ₂	0 °C	2.5	41
3	PdCl ₂	rt	5	95
4	(PPh ₃) ₂ PdCl ₂	rt	24	0
5	(COD)PdCl ₂	rt	24	0
6	Pd(OAc) ₂	rt	24	0

^a100 μ L of MeCN were added to the reaction mixture.

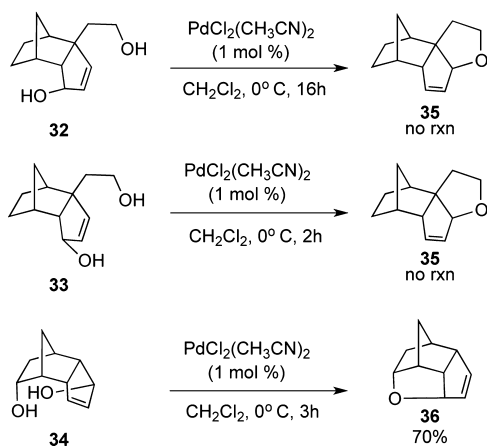
reaction conditions⁷ using PdCl₂(MeCN)₂ as the precatalyst, whereby **31** was isolated in 92% yield. In entry 2, acetonitrile was added to the reaction mixture to inhibit precatalytic loss of MeCN. In the event, as would be predicted, the reaction conversion drastically decreases to below 50% of the standard reaction conditions. Interestingly, when PdCl₂ was employed (no acetonitrile present), the reaction proceeded, but this required twice the standard catalyst loading and an elevated temperature. This may be due to the higher barriers or to the formation of polymeric Pd species that are deleterious to catalysis. With more coordinating ligands such as PPh₃ or the bidentate COD, the reactivity is reduced and in these cases (entries 4, 5) or with palladium acetate (entry 6), no reaction is observed.

To compare the possibility of *syn*-addition versus *anti*-addition, as well as the necessity for hydrogen bonding, bicyclic compounds **32**–**34** were designed and synthesized.^{11b} Our initial hypothesis based on the mechanism of cyclization and dehydration of acyclic compounds, using **32** as a substrate for the reaction to proceed there must be no necessity for hydrogen bonding as the two hydroxyl groups possess a *trans* relationship. In addition, if the reaction proceeds it would likely involve a novel *syn*-addition, *anti*-elimination or *anti*-addition, *syn*-elimination mechanism. Importantly, under Au(I) conditions bicyclic compound **32** did not cyclize.^{11b} Both compounds **33** and **34** have the ability to hydrogen bond. However, **33** might be expected to favor a *syn*-addition, *syn*-elimination over an *anti*-addition, *anti*-elimination mechanism with the catalyst coordinating on the *exo* face. Compound **34** was designed because it would be expected to favor an *anti*-addition, *anti*-elimination mechanism with the catalyst on the *exo* face.



Compounds **32**–**34** were treated under the standard reaction conditions, and the results are summarized in Scheme 9. When **32** and **33** were allowed to react at 0 °C, even after a prolonged reaction time, none of the cyclized product **35** was observed. This is not surprising given that only *anti*-addition, *anti*-elimination mechanisms without steric hindrance showed low energy reaction pathways for acyclic compounds. In good agreement with the calculations, substrate **34**, designed to favor *anti*-addition, *anti*-elimination did indeed undergo reaction at 0 °C to form **36** in 70% yield after 3h.

Scheme 9. Reaction of Bicyclic Probes **32**–**34**



Much to our surprise, **32** and **33** could be encouraged to cyclize by increasing the temperature and reaction time (Table 2, entries 1, 2). Also, when the substrates were treated with anhydrous HCl generated *in situ* from acetyl chloride and methanol, **35** was again produced. Under HCl conditions the yield of **35** from **32** is >65% in 1 h, while under Pd conditions the yield is 81% in 6 h. This suggests that under normal conditions Pd catalysis is likely, but formation of small concentrations of HCl cannot be ruled out. To examine the

Table 2. Cyclization of Bicyclic Compounds **32** and **33**

entry	substrate	conditions ^a	time (h)	yield (%)
1	32	1	6	81
2	33	1	2	94
3	32	2	1	66
4	33	2	1	86

^aConditions 1: PdCl₂(MeCN)₂ (3 mol %), CH₂Cl₂, rt. Conditions 2: CH₃COCl (5 mol %), MeOH (5 mol %), CH₂Cl₂, rt.

Pd catalyzed cyclization mechanisms of bicyclic compounds **32**–**34** computational analysis was undertaken.

Computational Evaluation of Bicyclic Systems. As expected, computational analysis of compound **34** revealed a low energy *anti*-addition, *anti*-elimination pathway for cyclization and dehydration. Figure 5 shows the *anti*-addition

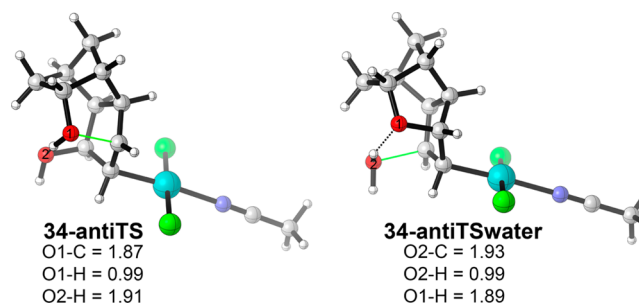


Figure 5. Cyclization and dehydration transition states for bicyclic compounds **34**. Bond lengths reported in Å.

transition state, **34-antiTS**, with $\Delta H^\ddagger = 2.9$ kcal/mol ($\Delta G^\ddagger = 4.6$ kcal/mol) relative to the ground state PdCl₂(MeCN)(**34**) π complex. The barrier for Pd-catalyzed cyclization of **34** is lower in energy than for monoallylic diol **A** because cyclization results in a five-membered rather than six-membered ring. In this system the diol hydrogen bonding allows direct intramolecular proton transfer and subsequent water loss. The water dissociation transition state, **34-antiTSwater**, is shown in Figure 5. In contrast to the acyclic monoallylic diol systems, the water dissociation barrier controls the rate of catalytic turnover. The ΔH^\ddagger and ΔG^\ddagger for **34-antiTSwater** are 8.6 and 10.3 kcal/mol respectively. These barriers are consistent with high yielding product formation found experimentally.

For compound **33**, stepwise *syn*-addition, *syn*-elimination and *anti*-addition, *anti*-elimination pathways are both possible. Due to the steric crowding of the bicyclic carbon framework, the *syn*-addition transition state, **33-synTS**, is several kcal/mol lower in energy than *anti*-addition. **33-synTS**, shown in Figure 6, has $\Delta H^\ddagger = 8.8$ kcal/mol ($\Delta G^\ddagger = 9.6$ kcal/mol). Although in **33-synTS** the diols are prevented from hydrogen bonding, the resulting intermediate has sufficient flexibility to allow the Pd–C σ -bond to twist out of the way and allow for intramolecular diol hydrogen bonding and proton transfer. After proton transfer, water release via transition state **33-synTSwater** requires $\Delta H^\ddagger = 8.4$ kcal/mol ($\Delta G^\ddagger = 9.2$ kcal/mol). This *syn*-addition, *syn*-elimination pathway is lower in energy than

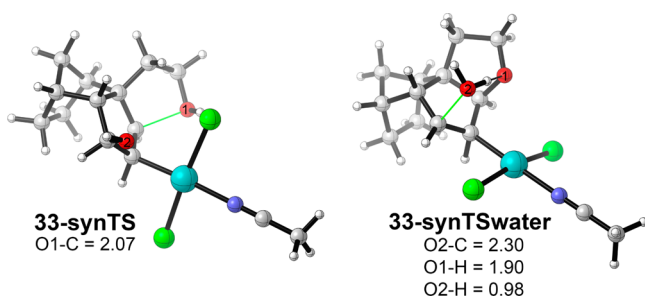


Figure 6. Cyclization and dehydration transition states for bicyclic compounds **33**. Bond lengths reported in Å.

pathways involving palladium hydroxide elimination or concerted S_N2' .

Bicyclic compound **32** represents an interesting example because due to the constraints of the substrate, a *syn*, *anti* or *anti*, *syn* pathway is needed, but this is not what is observed for acyclic systems. For **32**, there is the possibility to begin with either *syn*-addition or *anti*-addition (Scheme 10, Figure 7). The

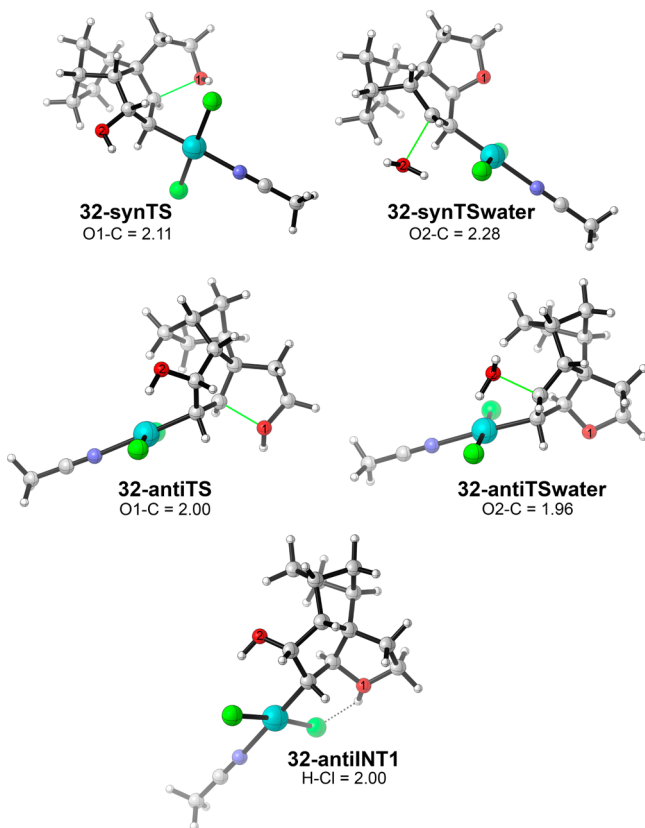


Figure 7. Cyclization and dehydration transition states for bicyclic compounds **32**. Bond lengths reported in Å.

syn-addition transition state (**32-synTS**) has a low $\Delta H^\ddagger = 9.2$ kcal/mol ($\Delta G^\ddagger = 9.8$ kcal/mol) to give **32-synINT1** that is slightly exothermic. Because no direct proton transfer can occur between diol groups and there is also no possibility for *syn* Pd(OH) elimination, the palladium chloride ligand mediates proton transfer, resulting in the intermediate **32-synINT2**. Proton transfer to the palladium chloride ligand to give coordinated HCl requires $\Delta H = 15.4$ kcal/mol. Subsequent proton shuttling to the allylic hydroxyl group to give **synINT3** has $\Delta H = 4.1$ kcal/mol. Finally, loss of water via transition state

32-synTSwater has $\Delta H^\ddagger = 21.0$ kcal/mol ($\Delta G^\ddagger = 21.1$ kcal/mol). This transition state features an *anti*-relationship between the water and Pd (Figure 7).

Alternative to the *syn*-addition pathway outlined above, an *anti*-addition pathway is also possible. As expected, the bicyclic carbon framework disfavors the *anti*-addition transition state, **32-antiTS**, compared **32-synTS** because of the *endo*-positioning of the catalyst. The ΔH^\ddagger for **32-antiTS** is 15.6 kcal/mol ($\Delta G^\ddagger = 16.8$ kcal/mol). For the resulting intermediate **32-antiINT1**, $\Delta H = 6.2$ kcal/mol. With linear Au(I) catalysts there is no viable pathway for proton transfer between diol groups after *anti*-addition and therefore no cyclization product was experimentally observed.^{11b} In contrast, the geometry of intermediate **32-antiINT1** (see Figure 7) allows proton transfer using a palladium chloride ligand to give intermediate **32-antiINT2** and requires $\Delta H = 17.5$ kcal/mol. It is also possible that adventitious water can direct proton shuttling, but the thermodynamics for this process are slightly higher in energy than chloride ligand mediated proton shuttling. For subsequent proton transfer to the allylic hydroxyl group, $\Delta H = 10.1$ kcal/mol. For subsequent water loss via **32-antiTSwater**, $\Delta H^\ddagger = 18.3$ ($\Delta G^\ddagger = 19.3$ kcal/mol). Comparison of the enthalpy and free energy surfaces in Scheme 10 suggests that Pd-catalyzed cyclization and dehydration of compound **32** likely proceeds via an *anti*-addition, *syn*-elimination mechanism. This mechanism is also lower in energy than concerted S_N2' transition states that have barriers generally greater than 30 kcal/mol (see Supporting Information). This mechanism is also ~ 6 kcal/mol lower in energy than transition states involving two Pd catalysts (see Supporting Information).

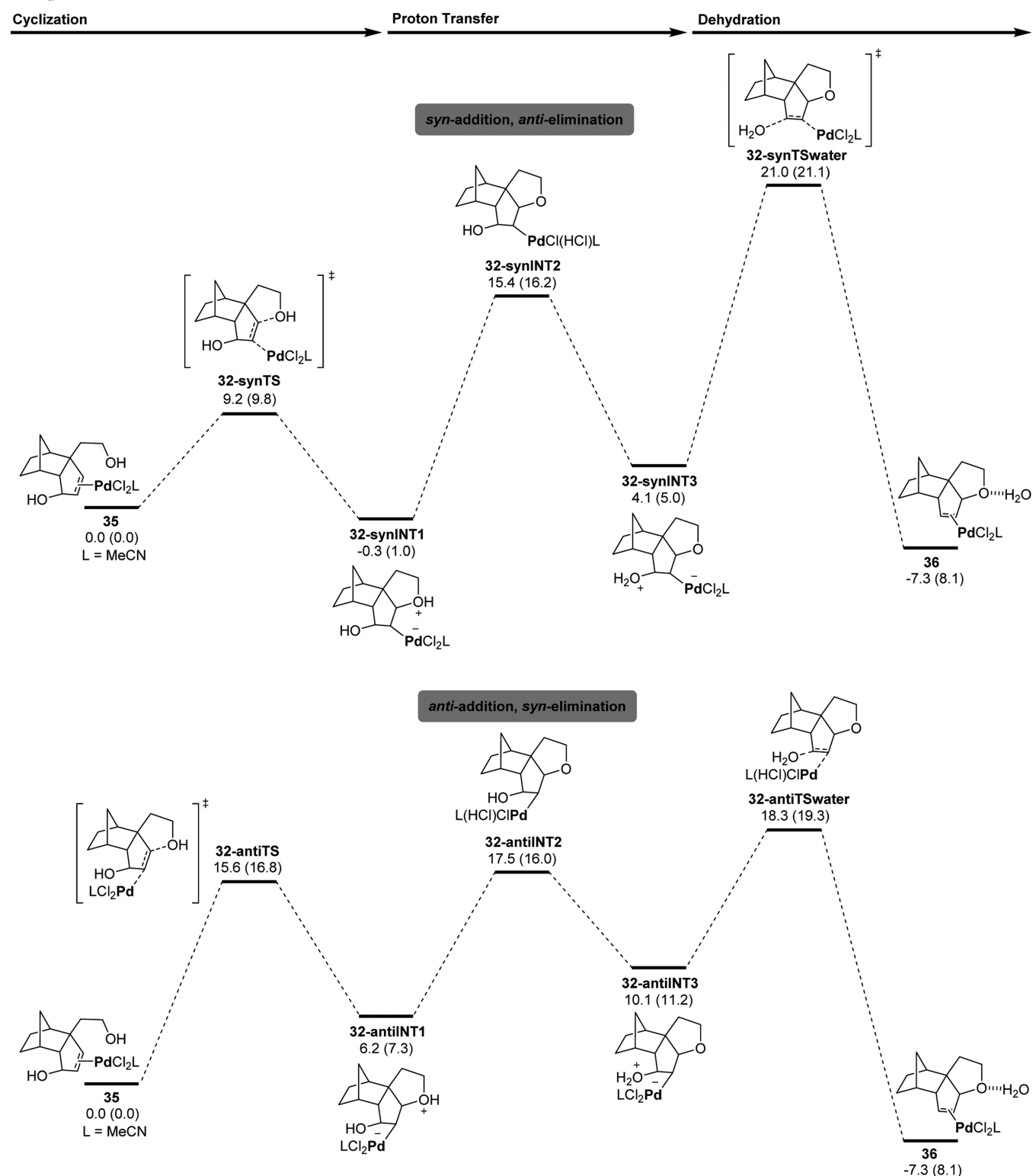
In both the *anti*-addition and *syn*-addition pathways a $PdL_2(HCl)$ intermediate is formed. In addition to Pd-catalysis, it is also possible that HCl dissociates and catalyzes further cyclization and dehydration. However, the barrier for subsequent water loss is less than 1 kcal/mol higher in energy than the energy to form the $PdL_2(HCl)$ intermediate. This suggests that Pd-catalysis and HCl catalysis may occur simultaneously for the reaction with compound **32**.

CONCLUSION

In conclusion, DFT calculations and experiments were combined to show that acyclic monoallylic diol cyclization and dehydration (S_N2') are catalyzed by $PdCl_2(MeCN)$, which occurs via an *anti*-addition, *anti*-elimination pathway. Pd-catalysis provides the same general mechanism for chirality transfer during cyclization and dehydration as was proposed for Au-catalyzed reactions.¹¹ Under normal catalytic conditions with acyclic systems, HCl formation and catalysis are unlikely. For bicyclic compounds, in contrast to Au catalysis, Pd-catalysis allows the possibility for either (i) *anti*-addition, *anti*-elimination, (ii) *syn*-addition, *syn*-elimination, or (iii) *anti*-addition, *syn*-elimination. These findings suggest that both Pd- and Au-catalyzed reactions have specific systems for which they may be optimal, with Pd-catalyzed reactions offering alternative pathways on difficult substrates.

Computational Methodology. All calculations were carried out in Gaussian 09¹⁷ using the M06 density functional.¹⁸ The structures reported are minima or first-order saddle points and confirmed by normal-mode vibration analysis. For Pd the LANL2DZ basis set was used. All other atoms were modeled with the 6-31G(d,p) basis set. Test calculations showed very small energy changes for larger basis sets. All optimizations were performed in THF or CH_2Cl_2

Scheme 10. Enthalpy (Free Energy) Reaction Coordinate Diagram for Cyclization, Proton Transfer, and Dehydration of Compound 32 (kcal/mol)



solvent using the SMD¹⁹ solvent parameters implemented in Gaussian 09 to estimate ΔG_{soln} . All enthalpies and free energies are reported at the standard state.

EXPERIMENTAL SECTION

General Experimental Methods. All reactions were carried out under an atmosphere of nitrogen. Anhydrous solvents were transferred

via syringe to flame-dried glassware, which had been cooled under a stream of dry nitrogen. Anhydrous tetrahydrofuran (THF), acetonitrile, and dichloromethane were dried using a solvent purification system. Analytical thin layer chromatography (TLC) was performed using 250 μm silica gel 60 F254 pre-coated plates. Flash column chromatography was performed using 230–400 Mesh 60 Å silica gel. The eluents employed are reported as volume/volume percentages. Melting points were recorded on a capillary melting point apparatus.

Nuclear magnetic spectra (^1H NMR and ^{13}C NMR) were recorded on 500 and 300 MHz spectrometers. Infrared spectra were obtained on a spectrometer at 0.5 cm^{-1} resolution. Compounds **30**, **31**, **32**, **33**, **34**, **35**, and **36** have been described in the literature and when prepared here satisfactorily matched all previously reported data.^{10a,11b}

General Procedure for the Pd-Catalyzed Cyclization Reactions (Table 1). The palladium catalyst (10 mol %) was added at 0°C to a 5 mL vial containing a solution of diol **30** in THF (0.1 M) and was stirred at the same temperature. When TLC analysis indicated complete consumption of the starting material, the reaction mixture was diluted with CH_2Cl_2 and filtered through a short plug of silica. The solution of crude product was concentrated and purified by flash chromatography (5% EtOAc/hexanes) to give the product as a colorless oil.

General Procedure for the Pd-Catalyzed Cyclization Reactions (Scheme 9). $\text{PdCl}_2(\text{CH}_3\text{CN})_2$ (1 mol %) was added at 0°C to a 5 mL vial containing a solution of substrate in CH_2Cl_2 (0.1 M) and was stirred at the same temperature. When TLC analysis indicated complete consumption of the starting material, the reaction mixture was diluted with CH_2Cl_2 and filtered through a short plug of silica. The solution of crude product was concentrated and purified by flash chromatography (5% EtOAc/hexanes) to give the product as a colorless oil.

General Procedure for the HCl Acid-Catalyzed Cyclization Reactions (Table 2). Acetyl chloride (100 μL , 1.41 mmol) was added to MeOH (60 μL , 1.48 μmol) in CH_2Cl_2 (12 mL) and stirred for 5 min to prepare a stock solution of anhydrous HCl. An aliquot of this solution (5 mol % relative to **32**) was then added to a solution of substrate in CH_2Cl_2 (0.1 M). After TLC analysis indicated complete consumption of the starting material, the reaction mixture was concentrated and then purified by flash chromatography (5% EtOAc/hexanes) to give the product as a colorless oil.

■ ASSOCIATED CONTENT

■ Supporting Information

Full ref 17 and xyz coordinates. This material is available free of charge via the Internet at <http://pubs.acs.org>.

■ AUTHOR INFORMATION

Corresponding Author

*E-mail: dhe@chem.byu.edu; aponick@chem.ufl.edu.

Notes

The authors declare no competing financial interest.

■ ACKNOWLEDGMENTS

D.H.E. thanks Brigham Young University (BYU) and the Fulton Supercomputing Lab (FSL) for computational support. A.A. thanks the Herman Frasch Foundation (647-HF07) and the James and Ester King Biomedical Research Program (09KN-01) for their generous support of our programs.

■ REFERENCES

- (1) Yamamoto, H. *Lewis Acids in Organic Synthesis*, Vols. 1 and 2; Wiley-VCH: Weinheim, Germany, 2000.
- (2) (a) Jørgensen, K. A. *Synthesis* **2003**, 1117. (b) Corma, A.; Garcia, H. *Chem. Rev.* **2003**, *103*, 4307. (c) Bandini, M.; Melloni, A.; Tommasi, S.; Umani-Ronchi, A. *Synlett* **2005**, 1199. (d) Poulsen, T.; Jørgensen, K. A. *Chem. Rev.* **2008**, *108*, 2903. (e) Rueping, M.; Nachtsheim, B. J. *Beilstein J. Org. Chem.* **2010**, *6*, 6. (f) Zen, M.; You, S.-L. *Synlett* **2010**, 1289.
- (3) (a) Kagan, H. B.; Riant, O. *Chem. Rev.* **1992**, *92*, 1007. (b) Pindur, U.; Lutz, G.; Otto, C. *Chem. Rev.* **1993**, *93*, 741. (c) Carmona, D.; Lamata, M. P.; Oro, L. A. *Coord. Chem. Rev.* **2000**, *200*, 717. (d) Corey, E. J. *Angew. Chem., Int. Ed.* **2002**, *41*, 1650. (e) Raymond, S.; Cossy, J. *Chem. Rev.* **2008**, *108*, 5359.
- (4) (a) Nakamura, I.; Yamamoto, Y. *Chem. Rev.* **2004**, *104*, 2127. (b) Kirsch, S. F. *Synthesis* **2008**, 3183. (c) Lee, S. I.; Chatani, N. *Chem.*

Commun. **2009**, 371. (d) Tobisu, M.; Nakai, H.; Chatani, N. *J. Org. Chem.* **2009**, *74*, 5471. (e) Leung, J. C.; Krische, M. J. *Chem. Sci.* **2012**, *3*, 2202.

(5) (a) Hegedus, L. S. In *Organometallics in Synthesis*, 2nd ed.; Schlosser, M., Ed.; John Wiley and Sons: New York, 2002; pp 1123–1217. (b) Hosokawa, T.; Murahashi, S.-I. Intramolecular Oxy-palladation. In *Handbook of Organopalladium Chemistry for Organic Synthesis*; Negishi, E.-i., Ed.; John Wiley and Sons: New York, 2002; Vol. 2, pp 2169–2192. (c) Fürstner, A.; Davies, P. W. *Angew. Chem., Int. Ed.* **2007**, *46*, 3410. (d) Fürstner, A. *Chem. Soc. Rev.* **2009**, *38*, 3208. (e) Hashmi, A. S. K. *Angew. Chem., Int. Ed.* **2010**, *49*, 5232. (f) Shapiro, N. D.; Toste, F. D. *Synlett* **2010**, 675. (g) Rudolph, M.; Hashmi, A. S. K. *Chem. Commun.* **2011**, 47, 6536. (h) Leyva-Pérez, A.; Sabater, M. J. *Chem. Rev.* **2011**, *111*, 1657. (i) Engelin, C. J.; Fristrup, P. *Molecules* **2011**, *16*, 951.

(6) (a) Pearson, R. G. *J. Am. Chem. Soc.* **1963**, *85*, 3533. (b) Pearson, R. G. *J. Chem. Educ.* **1968**, *45*, 581. (c) Pearson, R. G. *J. Chem. Educ.* **1968**, *45*, 643. (d) Pearson, R. G. *Inorg. Chim. Acta* **1995**, *240*, 93. (e) LoPachin, R. M.; Gavin, T.; DeCaprio, A.; Barber, D. S. *Chem. Res. Toxicol.* **2012**, *25*, 239.

(7) Uenishi, J.; Ohmi, M.; Ueda, A. *Tetrahedron: Asymmetry* **2005**, *16*, 1299.

(8) (a) Satoh, T.; Ikeda, M.; Miura, M.; Nomura, M. *J. Org. Chem.* **1997**, *62*, 4877. (b) Yang, S.-C.; Tsai, Y.-C. *Organometallics* **2001**, *20*, 763. (c) Ozawa, F.; Okamoto, H.; Kawagishi, S.; Yamamoto, S.; Minami, T.; Yoshifuji, M. *J. Am. Chem. Soc.* **2002**, *124*, 10968. (d) Kabalka, G. W.; Dong, G.; Venkataiah, B. *Org. Lett.* **2003**, *5*, 893. (e) Kinoshita, H.; Shinokubo, H.; Oshima, K. *Org. Lett.* **2004**, *6*, 4085. (f) Kawai, N.; Lagrange, J.-M.; Ohmi, M.; Uenishi, J. *J. Org. Chem.* **2006**, *71*, 4530. (g) Kawai, N.; Lagrange, J.-M.; Uenishi, J. *Eur. J. Org. Chem.* **2007**, 2808. (h) Utsunomiya, M.; Miyamoto, Y.; Ipposhi, J.; Ohshima, T.; Mashima, K. *Org. Lett.* **2007**, *9*, 3371. (i) Qin, H.; Yamagiwa, N.; Matsunaga, S.; Shibasaki, M. *Angew. Chem., Int. Ed.* **2007**, *46*, 409. (j) Uenishi, J.; Vikhe, Y. S.; Kawai, N. *Chem.—Asian J.* **2008**, *3*, 473. (k) Mora, G.; Piechaczyk, O.; Houdard, R.; Mézailles, N.; Le Goff, X.-F.; Le Floch, P. *Chem.—Eur. J.* **2008**, *14*, 10047. (l) Zaitsev, A. B.; Gruber, S.; Plüss, P. A.; Pregosin, P. S.; Veiros, Wörle, M. *J. Am. Chem. Soc.* **2008**, *130*, 11604. (m) Ohshima, T.; Miyamoto, Y.; Yasuhito, J.; Nakahara, Y.; Utsunomiya, M.; Mashima, K. *J. Am. Chem. Soc.* **2009**, *131*, 14317. (n) van Rijn, J. A.; Lutz, M.; von Chrzanowski, L. S.; Spek, L. A.; Bouwman, E.; Drent, E. *Adv. Synth. Catal.* **2009**, *351*, 1637. (o) Tanaka, S.; Seki, T.; Kitamura, M. *Angew. Chem., Int. Ed.* **2009**, *48*, 8948. (p) Guérinot, A.; Serra-Muns, A.; Gnam, C.; Bensoussan, C.; Reymond, S.; Cossy, J. *Org. Lett.* **2010**, *12*, 1808. (q) Miyata, K.; Katsuna, H.; Kawakami, S.; Kitamura, M. *Angew. Chem., Int. Ed.* **2011**, *50*, 4649. (r) Miyata, K.; Kitamura, M. *Synthesis* **2012**, *44*, 2138.

(9) Ketcham, J. M.; Aponick, A. *Top. Heterocycl. Chem.* **2013**, *32*, 157.

(10) (a) Aponick, A.; Li, C.-Y.; Biannic, B. A. *Org. Lett.* **2008**, *10*, 669. (b) Aponick, A.; Biannic, B. *Synthesis* **2008**, *20*, 3356. (c) Biannic, B.; Aponick, A. *Eur. J. Org. Chem.* **2011**, 6605. (d) Aponick, A.; Li, C.-Y.; Palmes, J. A. *Org. Lett.* **2009**, *11*, 121. (e) Aponick, A.; Li, C.-Y.; Malinge, J.; Marques, E. F. *Org. Lett.* **2009**, *11*, 4624. (f) Aponick, A.; Biannic, B.; Jong, M. R. *Chem. Commun.* **2010**, 46, 6849.

(11) (a) Aponick, A.; Biannic, B. *Org. Lett.* **2011**, *13*, 1330. (b) Ghebregiorgis, T.; Biannic, B.; Kirk, B. H.; Ess, D. H.; Aponick, A. *J. Am. Chem. Soc.* **2012**, *134*, 16307.

(12) (a) Fañanás-Mastral, M.; Aznar, F. *Organometallics* **2009**, *28*, 666. (b) Frémont, P.; Marion, N.; Nolan, S. P. *J. Organomet. Chem.* **2009**, *694*, 551. (c) Wu, J.; Kroll, P.; Dias, H. V. R. *Inorg. Chem.* **2009**, *48*, 423. (d) Brown, T. J.; Dickens, M. G.; Widenhoefer, R. A. *Chem. Commun.* **2009**, 6451.

(13) (a) Abraham, C. J.; Paull, D. H.; Bekele, T.; Scerba, M. T.; Dudding, T.; Lectka, T. *J. Am. Chem. Soc.* **2008**, *130*, 17085. (b) Vyas, D. J.; Larionov, E.; Besnard, C.; Guénee, L.; Mazet, C. *J. Am. Chem. Soc.* **2013**, *135*, 6177.

(14) (a) James, D. E.; Hines, L. F.; Stille, J. K. *J. Am. Chem. Soc.* **1976**, *98*, 1806. (b) Bäckvall, J.-E.; Åkermark, B.; Ljunggren, S. O. *J. Chem. Soc., Chem. Commun.* **1977**, 264. (c) Majima, T.; Kurosawa, H. *J. Chem.*

- Soc., Chem. Commun.* **1977**, 610. (d) Stille, J. K.; Divakaruni, R. *J. Am. Chem. Soc.* **1978**, *100*, 1303. (e) Bäckvall, J.-E.; Åkermark, B.; Ljunggren, S. O. *J. Am. Chem. Soc.* **1979**, *101*, 2411. (f) Hamed, O.; Henry, P. M.; Thompson, C. *J. Org. Chem.* **1999**, *64*, 7745. (g) ten Brink, G.-J.; Arends, I. W. C. E.; Papadogianakis, G.; Sheldon, R. A. *Appl. Catal., A* **2000**, *194–195*, 435. (h) Nelson, D. J.; Li, R.; Brammer, C. *J. Am. Chem. Soc.* **2001**, *123*, 1564. (i) Hayashi, T.; Yamasaki, K.; Mimura, M.; Uozumi, Y. *J. Am. Chem. Soc.* **2004**, *126*, 3036.
- (15) Ye, X.; Liu, G.; Popp, B. V.; Stahl, S. S. *J. Org. Chem.* **2011**, *76*, 1031.
- (16) (a) Vikhe, Y. S.; Hande, S. M.; Kawai, N.; Uenishi, J. *J. Org. Chem.* **2009**, *74*, 5174. (b) Wolfe, J. P.; Rossi, M. A. *J. Am. Chem. Soc.* **2004**, *126*, 1620. (c) Hay, M. B.; Wolfe, J. P. *J. Am. Chem. Soc.* **2005**, *127*, 16468. (d) Nakhla, J. S.; Kampf, J. W.; Wolfe, J. P. *J. Am. Chem. Soc.* **2006**, *128*, 2893.
- (17) Frisch, M. J. et al. *Gaussian 09*, revision B.01; Gaussian, Inc.: Wallingford, CT, 2009.
- (18) (a) Zhao, Y.; Truhlar, D. G. *Theor. Chem. Acc.* **2008**, *120*, 215. (b) Zhao, Y.; Truhlar, D. G. *Acc. Chem. Res.* **2008**, *41*, 157.
- (19) Marenich, A. V.; Cramer, C. J.; Truhlar, D. G. *J. Phys. Chem. B* **2009**, *113*, 6378.